Supplementary Materials for

Neutrophils Disturb Pulmonary Microcirculation in Sepsis-induced Acute Lung Injury

Inwon Park, Mingyo Kim, Kibaek Choe, Eunjoo Song, Howon Seo, Yoonha Hwang, Jinhyo Ahn, Seung-Hyo Lee, Jae Hyuk Lee, You Hwan Jo, Kyuseok Kim, Gou Young Koh*, and Pilhan Kim*

*Corresponding authors. E-mail: pilhan.kim@kaist.ac.kr (P.K.); gykoh@kaist.ac.kr (G.Y.K.)

This material includes:

Supplementary Materials

Supplementary Video 4. Increased neutrophil entrapment induces capillary obstruction in sepsis-induced ALI model.

Supplementary Video 5. Alteration of neutrophil dynamics in sepsis-induced ALI model.

Supplementary Video 6. Neutrophils block capillary and trigger dead space formation in sepsis-induced ALI model.

Supplementary Video 7. Neutrophils induce cluster formation *in situ* in the arteriole in sepsis-induced ALI model.

Supplementary Video 8. Capillary and arteriole obstruction of neutrophil aggregates induces dead space formation in sepsis-induced ALI model.

Supplementary Video 9. Depletion of neutrophil increases FCR of pulmonary microcirculation.

Supplementary Video 10. Abciximab improves pulmonary microcirculation in sepsis-induced ALI model.

Materials & Methods

Animal Model

To generate sepsis-induced ARDS model, high-dose LPS or CLP model was utilized. For high-dose LPS model, LPS (10mg/kg, *E. coli* serotype 055:B5, L2880, Sigma-Aldrich) was intraperitoneally administered to peritoneum before 3 to 6 hours of imaging. In the control group, the same amount of PBS was injected into the peritoneum. High-grade CLP was performed by a single experienced operator according to the previously described method [45]. 75% of the cecum was ligated with 6-0 black silk, and single puncture with a dual hole in distal cecum was made with a 21-gauge needle. After puncture, the cecum was gently squeezed to confirm the patency of puncture hole for extrusion of feces. The cecum was replaced to the abdominal cavity, and abdominal incision was closed with 4-0 black silk. The sham group underwent the same surgical procedure except for the cecal ligation and puncture.

Fluorescent dye and antibody utilized in intravital imaging

Erythrocyte was acquired by cardiac puncture and then labeled with Vybrant DiD (V22887, ThermoFisher Scientific) following the method described in product information sheet. 50 million counts of DiD-labeled erythrocyte was injected via a vascular catheter in tail vein right before imaging [46]. To visualize the vessel with a fluorescent dye, FITC (Molecular Weight 2M Da, Sigma-Aldrich) or Tetramethylrhodamine (TMR) conjugated dextran dye (Molecular Weight 40 KDa, ThermoFisher Scientific) was injected via same vascular catheter described above. To specifically label the neutrophil *in vivo*, 25 μg of Anti-Ly6G+ monoclonal antibody (Clone 1A8, 551459, BD) conjugated with a fluorophore Alexa Fluor 555 or 647 (A-20005 / A-20006, ThermoFisher Scientific) was injected via tail vein 2 hours before imaging. To visualize the

molecular expression of pulmonary sequestered neutrophil *in vivo*, 25 μg of CD11b (Clone M1/70, 553307, BD Biosciences) and CD18 (Clone GAME-46, 555280, BD Biosciences) conjugated with Alexa 555 was injected via tail vein 2 hours before imaging. DHE was prepared in a manner written in previous intravital studies except for higher dosages (10 mg/kg) [47]. For neutrophil depletion model, 200 μg of Anti-Ly6G monoclonal antibody (Clone 1A8, 551459, BD Biosciences) was injected intraperitoneally 24 hours before sepsis-induced ARDS modeling [48]. For Mac-1 inhibitor model, Anti-CD11b [49] (5 mg/kg, Clone M1/70, 553307, BD Biosciences) and Abciximab [50, 51] (10 mg/kg, Clotinab, ISU Abxis) were injected intraperitoneally 1 hour after CLP modeling which was 5 hours before intravital imaging. To compare the pre-abciximab and post-abciximab FCR, intravital imaging was performed 6 hours after CLP, and FCR imaging of pre-abciximab setting was acquired, and then abciximab was injected. At 30 minutes after the abciximab injection, FCR imaging of post-abciximab was performed.

Flow Cytometry

For flow cytometry analysis, neutrophil was isolated from blood collected from left ventricle and lung. To isolate pulmonary sequestered neutrophils, lungs were harvested and digested without perfusion. Lungs were placed in PBS solution, minced and filtered through a 40μm filter and stained with antibody for 30 minutes at 4°C. Antibody clones used in this studies: Ly6G-FITC (1A8, 551460, BD Biosciences), CD11a-BV510 (M17/4, 563669, BD Biosciences) CD11b-PE-Cy7 (M1/70, 552850, BD Biosciences), CD18-APC (C71/16, 562828, BD Biosciences), CD62L (MEL-14, 560514, BD Biosciences), Viability Dye eFluor 506 (65-0866-14, ThermoFisher Scientific). Stained cells were analyzed with LSR Fortessa flow cytometer (BD Biosciences). Analysis for flow cytometry was performed with Flowjo (FlowJo, LLC)

Histological Analysis

To validate neutrophil depletion in the lung of $LysM^{GFP/+}$ mouse, lungs were harvested after intravital imaging. Perfusion and fixation with 4% paraformaldehyde were performed and further fixed overnight in 4% paraformaldehyde. For hematoxylin and eosin (H&E) staining, tissues were processed using standard procedures, embedded in paraffin, and sliced into 4μm sections followed by conventional H&E staining.

Arterial Blood Gas Analysis

To assess the partial pressure of O_2 and CO_2 in arterial blood to evaluate the oxygenation status, arterial blood gas analysis was performed. 1ml syringe with 22 gauge needle was coated with heparin and introduced into a left ventricle of the heart. Approximately 200 μl of blood was sampled and analyzed with i-STAT handheld blood analyzer (G3 cartridge, Abbott Point of Care Inc). Animals were euthanized with CO_2 chamber right after blood sampling.

Wet-to-dry weight Ratio

To assess the pulmonary edema in mice, the wet-to-dry weight ratio was performed. At 6 hours and 24 hours of injury with the Mac-1 inhibitor experimental model described as above, the entire unlavaged lung was harvested and immediately weighed (wet weight) and reweighed after keeping in a 60 °C drying oven for 72 hours (dry weight).

Imaging System

To visualize *in vivo* pulmonary microcirculation through the window, a custom-built video-rate laser-scanning confocal microscopy system was implemented [52-56]. Three continuous laser modules (Wavelength at 488 nm (MLD488, Cobolt), 561 nm (Jive, Cobolt), and 640 nm (MLD640, Cobolt)) were utilized as excitation light source for multi-color fluorescence imaging. Laser beams were collinearly integrated by dichroic beam splitters (DBS1; FF593-Di03, DBS2; FF520-Di02, Semrock) and transferred to the laser-beam scanner by a multi-edge dichroic beam splitter (DBS3; Di01-R405/488/561/635, Semrock). The laser scanning section consisted of 2 axises - X-axis scanning with a rotating polygonal mirror with 36 facets (MC-5, aluminum coated, Lincoln Laser) and Y-axis scanning with a galvanometer scanning mirror (6230H, Cambridge Technology). The two-dimensional raster scanning laser beam was transferred to the lung of mice through the commercial objective lens (LUCPLFLN, 20X, NA 0.45, Olympus, LUCPLFLN, 40X, NA 0.6, Olympus, LCPLFLN100XLCD, 100X, NA 0.85, Olympus). The fluorescence signal emitted from the lung of the mice on XYZ translational 3D stage (3DMS, Sutter Instrument) were epi-detected by the objective lens. De-scanned three-color fluorescence signals were spectrally divided by a dichroic beam splitter (DBS4; FF560-Di01, DBS5; FF649-Di01, Semrock) and then detected by photomultiplier tubes (PMT; R9110, Hamamatsu) through bandpass filters (BPF1; FF02-525/50, BPF2; FF01-600/37, BPF3; FF01-685/40, Semrock). The voltage outputs of each PMTs were digitalized by a 3-channel frame grabber (Solios, Matrox) with 8-bit resolution at the sampling rate of 10 MHz. Using a custom-written imaging software based on Matrox Imaging Library (MIL9, Matrox) and Visual C#, video-rate movies were displayed and recorded in real time at the frame rate of 30Hz and frame size of 512 x 512 pixels.

Intravital Pulmonary Imaging

The detailed description is provided in the previous study [57]. All the mice were anesthetized with Ketamine (80 mg/kg) and Xylazine (12 mg/kg). After anesthesia, using a lightning guidewire, intubation with 20 Gauge vascular catheter was performed and connected to a mechanical ventilator (MouseVent, Kent Scientific). Ventilation was conducted in the setting of the inspiratory pressure of 24~30 mmHg, a respiratory rate of 120~130 breaths per minute, and a positive-end expiratory pressure of 2 cmH_2O. Isoflurane was delivered with 2% to maintain anesthesia status, and pulse oximetry was applied to monitor oxygenation and survival status. Thermal probe of the homeothermic system (RightTemp, Kent Scientific) was introduced into the rectum, and a feedback-regulated heating pad was used to maintain body temperature at 37.0 °C. Tail vein was cannulated with a 30-gauge needle attached to the PE-10 tube for intravenous injection of molecular dye and cell. Then mice were positioned in right lateral decubitus which was followed by dissection of left thoracotomy. Skin and muscle were dissected until rib exposure and incision was made between 3rd and 4th rib to exposure pleura. After thoracotomy, previously mentioned imaging window [58, 59] was applied to the surface of the pleura, and negative suction pressure (20~30 mmHg) provided by a pump (DOA-P704-AA, GAST) and regulator (NVC 2300a, EYELA) was applied via a tube connected to lung imaging window.

Image Processing

Images were displayed and stored at an acquisition rate of 30 frames per second with 512 x 512 pixels per frame. The real-time image frames were averaged over 30 frames by using a MATLAB (Mathworks) code to improve contrast and signal-to-noise ratio. To minimize the motion artifact, each frames were processed with image registration algorithm prior to averaging.

Functional capillary imaging analysis was performed using real-time movie of DiD-labeled erythrocytes flowing in capillaries. After splitting colors of movie, sequential images of channels detecting DiD was processed by a median filter with a radius of two pixels to enhance the signal-to-noise ratio. Maximal intensity projection of 600 to 900 (20 – 30 seconds) frames was generated to show the functional capillary perfused by erythrocytes. Functional capillary ratio (FCR) was determined by calculating the ratio of functional capillary area (DiD-labeled RBC) to the total capillary area (vessel area detected by Tie2 or Dextran signaling). All image processing to calculate FCR was performed by ImageJ (https://imagej.nih.gov/ij/). Image rendering with three-dimensional reconstruction, track analysis of erythrocytes and neutrophils, and plotting track displacement was conducted with IMARIS 8.2 (Bitplane).

Statistical Analysis

All data are presented as mean ± standard deviation (S.D.) or median ± interquartile range, as appropriate to represent values of the group respectively. Statistical differences between means or medians were determined by unpaired 2-tailed Student's t-test, Mann-Whitney test, one-way ANOVA with post hoc Holm-Sidak's multiple comparisons, or Kruskal-Wallis test with post hoc Dunn's multiple comparison tests, as appropriate. Statistical significance was set at $P < 0.05$, and analysis was performed with Prism 6.0 (GraphPad).

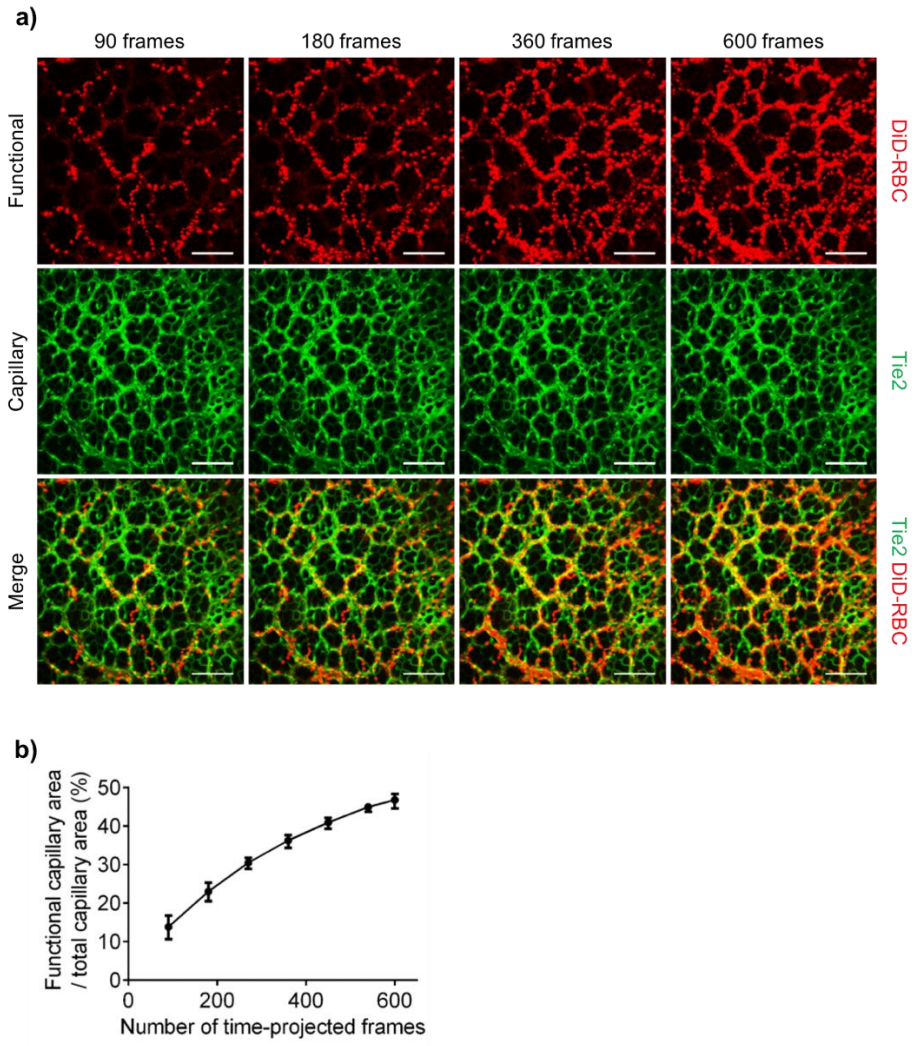

Supplementary Figure S1. Mapping of functional capillary ratio (FCR) according to number of frames.

(**a**) Representative image of functional capillary area revealed by perfusion of DiD-labeled erythrocyte, anatomical capillary revealed by Tie2+GFP+ endothelial cell, and merged image according to the number of maximally projected sequential frames. FCR was generated by calculating the area of anatomical capillary overlapped with the functional capillary area produced with maximal intensity projection of real-time sequential image of DiD-labeled erythrocyte. Scale bars, 100 μm. (**b**) Quantification of FCR in each time-projected frames (n = 5 per each group).

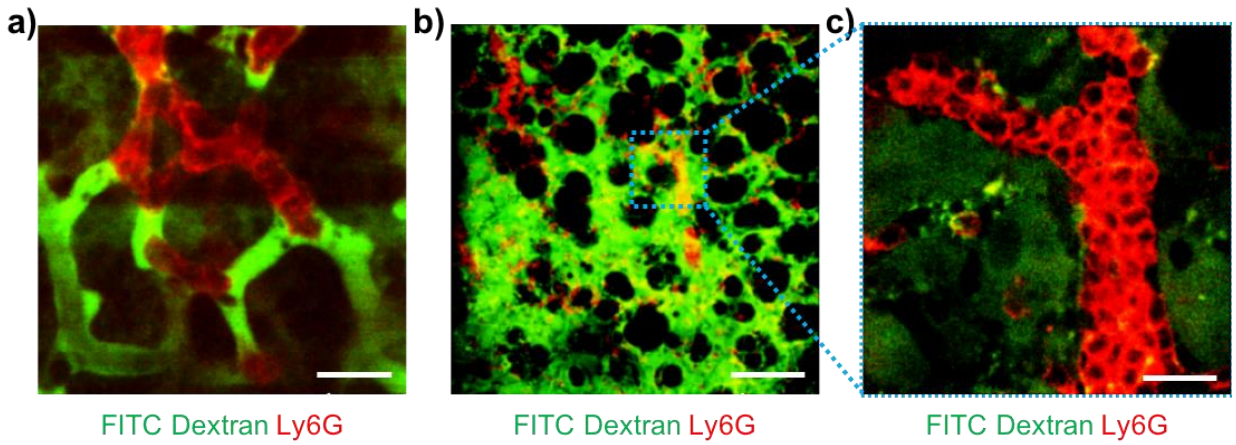

Supplementary Figure S2. Identification of neutrophil aggregates in capillary and arteriole. (**a**) Representative intravital lung imaging of thrombus formation inside capillary. Scale bar, 20 μm. (**b**) Representative intravital lung imaging of thrombus formation in arteriole and (**c**) magnified image in **b**. Scale bars, 100 μm in **b**, and 20 μm in **c**.

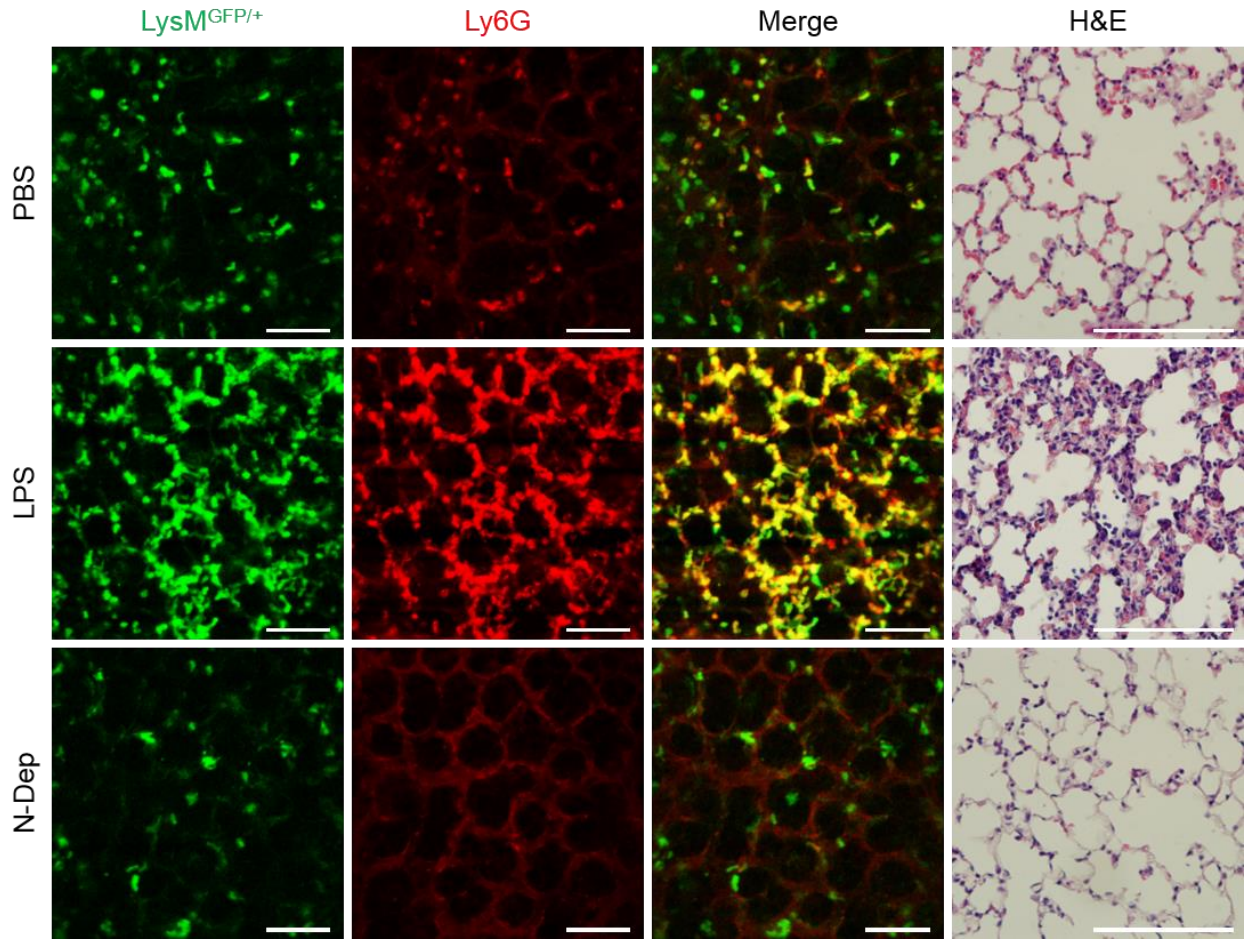

Supplementary Figure S3. Confirmation of neutrophil depletion in LysM$^{GFP/+}$ model.

Representative intravital imaging of neutrophil depletion in PBS and LPS and neutrophil depletion (N-Dep) group. Intravital imaging was performed 6 hours after intraperitoneal PBS or LPS injection. Intravital imaging of N-dep model was performed 24 hours after intraperitoneal high-dose of anti-Ly6G antibody injection. Neutrophil depletion was confirmed by intravital imaging and histological study of H&E section. Remnant LysM+ cell in N-dep model represents macrophage. Scale bars, 100 μm

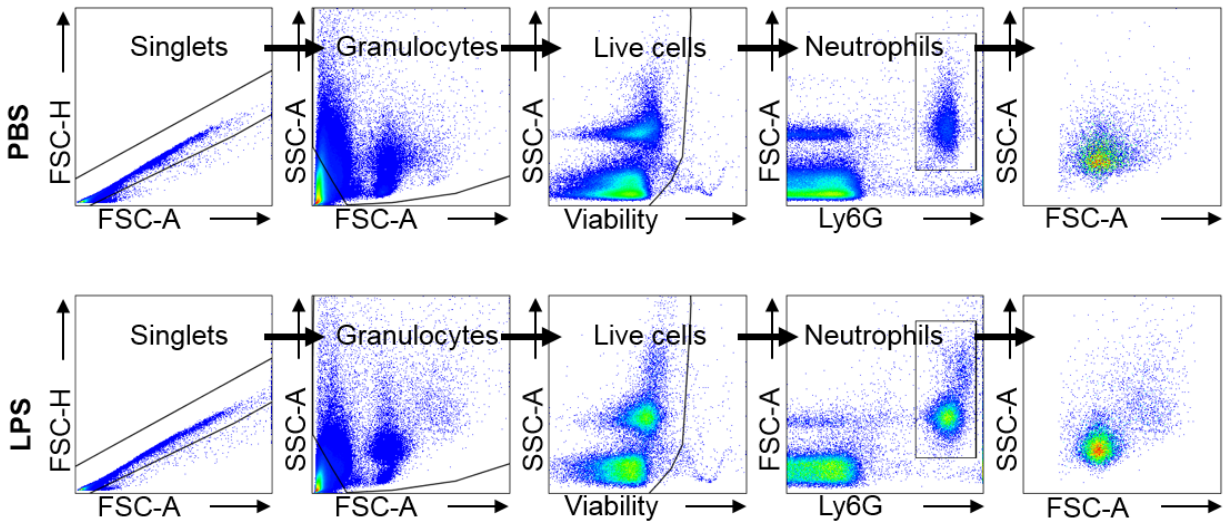

Supplementary Figure S4. Flow cytometry gating strategy to isolate neutrophil.

Representative flow cytometry gating strategy to identify surface expression of neutrophil in PBS and LPS group.

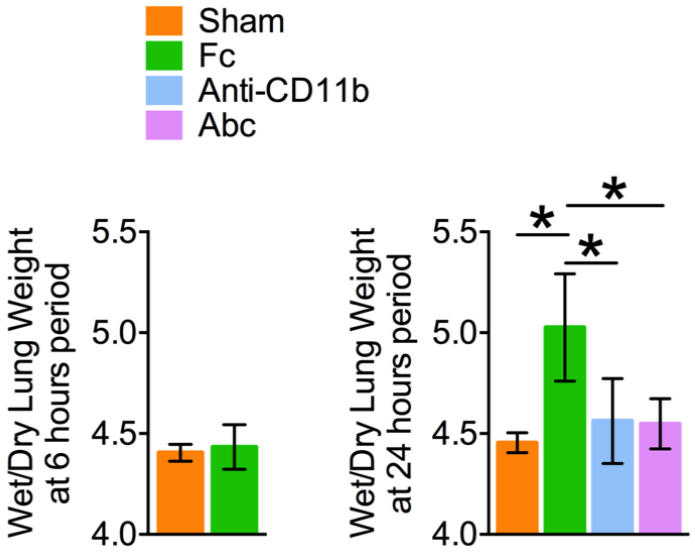

Supplementary Figure S5. Assessment of pulmonary edema in Mac-1 inhibition.

Comparisons of wet-to-dry weight ratios of the lung in sham, CLP, CLP with Anti-CD11b, and CLP with Abciximab treatment group at 6 and 24 hours after lung injury. Significant amelioration of lung edema by Mac-1 inhibition was identified at 24 hours after injury while no difference was identified at the early stage of injury (6 hours) [60, 61]. (n = 4 and 6 mice in 6 hours ; 5, 8, 4, and 7 mice in 24 hours, * $P < 0.05$, Mann-Whitney test). Data are means ± s.d..

Supplementary References

45. Rittirsch D, Huber-Lang MS, Flierl MA, Ward PA. Immunodesign of experimental sepsis by cecal ligation and puncture. *Nat Protoc* 2009: 4(1): 31-36.

46. Seo H, Hwang Y, Choe K, Kim P. In vivo quantitation of injected circulating tumor cells from great saphenous vein based on video-rate confocal microscopy. *Biomed Opt Express* 2015: 6(6): 2158-2167.

47. Finsterbusch M, Hall P, Li A, Devi S, Westhorpe CL, Kitching AR, Hickey MJ. Patrolling monocytes promote intravascular neutrophil activation and glomerular injury in the acutely inflamed glomerulus. *Proc Natl Acad Sci U S A* 2016: 113(35): E5172-5181.

48. Daley JM, Thomay AA, Connolly MD, Reichner JS, Albina JE. Use of Ly6G-specific monoclonal antibody to deplete neutrophils in mice. *J Leukoc Biol* 2008: 83(1): 64-70.

49. Ahn GO, Tseng D, Liao CH, Dorie MJ, Czechowicz A, Brown JM. Inhibition of Mac-1 (CD11b/CD18) enhances tumor response to radiation by reducing myeloid cell recruitment. *Proc Natl Acad Sci U S A* 2010: 107(18): 8363-8368.

50. Peter K, Schwarz M, Conradt C, Nordt T, Moser M, Kubler W, Bode C. Heparin inhibits ligand binding to the leukocyte integrin Mac-1 (CD11b/CD18). *Circulation* 1999: 100(14): 1533-1539.

51. Schwarz M, Nordt T, Bode C, Peter K. The GP IIb/IIIa inhibitor abciximab (c7E3) inhibits the binding of various ligands to the leukocyte integrin Mac-1 (CD11b/CD18, alphaMbeta2). *Thromb Res* 2002: 107(3-4): 121-128.

52. Rajadhyaksha M, Anderson RR, Webb RH. Video-rate confocal scanning laser microscope for imaging human tissues in vivo. *Appl Opt* 1999: 38(10): 2105-2115.

53. Veilleux I, Spencer JA, Biss DP, Cote D, Lin CP. In Vivo Cell Tracking With Video Rate Multimodality Laser Scanning Microscopy. *IEEE Journal of Selected Topics in Quantum Electronics* 2008: 14(1): 10-18.

54. Choe K, Jang JY, Park I, Kim Y, Ahn S, Park DY, Hong YK, Alitalo K, Koh GY, Kim P. Intravital imaging of intestinal lacteals unveils lipid drainage through contractility. *J Clin Invest* 2015: 125(11): 4042-4052.

55. Choe K, Hwang Y, Seo H, Kim P. In vivo high spatiotemporal resolution visualization of circulating T lymphocytes in high endothelial venules of lymph nodes. *J Biomed Opt* 2013: 18(3): 036005.

56. Ahn J, Choe K, Wang T, Hwang Y, Song E, Kim KH, Kim P. In vivo longitudinal cellular imaging of small intestine by side-view endomicroscopy. *Biomed Opt Express* 2015: 6(10): 3963-3972.

57. Park I, Choe K, Seo H, Hwang Y, Song E, Ahn J, Hwan Jo Y, Kim P. Intravital imaging of a pulmonary endothelial surface layer in a murine sepsis model. *Biomed Opt Express* 2018: 9(5): 2383-2393.

58. Looney MR, Thornton EE, Sen D, Lamm WJ, Glenny RW, Krummel MF. Stabilized imaging of immune surveillance in the mouse lung. *Nat Methods* 2011: 8(1): 91-96.

59. Lamm WJ, Bernard SL, Wagner WW, Jr., Glenny RW. Intravital microscopic observations of 15-microm microspheres lodging in the pulmonary microcirculation. *J Appl Physiol (1985)* 2005: 98(6): 2242-2248.

60. Carraway MS, Piantadosi CA, Jenkinson CP, Huang YC. Differential expression of arginase and iNOS in the lung in sepsis. *Exp Lung Res* 1998: 24(3): 253-268.

61. Wang Q, Wu X, Tong X, Zhang Z, Xu B, Zhou W. Xuebijing Ameliorates Sepsis-Induced Lung Injury by Downregulating HMGB1 and RAGE Expressions in Mice. *Evid Based Complement Alternat Med* 2015: 2015: 860259.